

Projection Clutching System for Force Transmission System based on Tulip-shaped Electrostatic Clutch

H. Sasaki, S. Takagi, M. Shikida and K. Sato,
 Dept. of Micro System Eng., Nagoya University,
 Furo-cho, Chikusa-ku, Nagoya, Japan

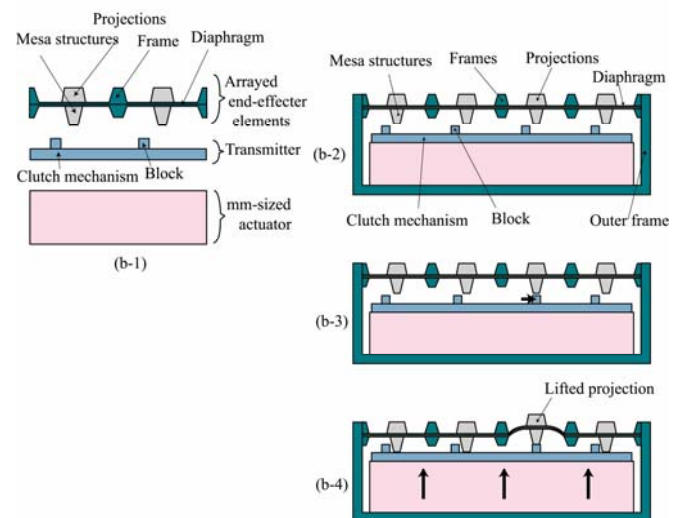
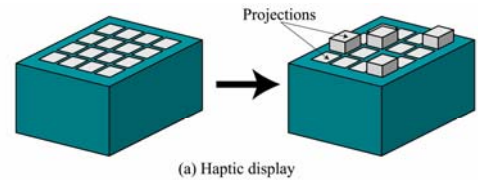
Abstract:

We have previously proposed an arrayed vertical motion system based on a tulip-shaped electrostatic clutch for producing haptic displays. The system has an advantage in that it is able to individually operate arrayed minute projection with high-power and large strokes (Output: 600 mN and displacement: 60 μ m). This time, We added a new electrostatic latch mechanism to the system to individually control the projection state. We used MEMS technologies to fabricate a 4x4 array electrostatic latch mechanism. The total size of the mechanism was 6.0 x 6.0 x 0.5 mm. We evaluated the relationship between the applied voltage and a holding force of a few mN was obtained for the spring device.

1. INTRODUCTION

Among the many types of micro-sized actuators have been proposed and applied to MEMS devices, and various types of power sources, such as electrostatic- [1-2], thermal- [2-7], magnetic- [8-9], piezo-electric- [10-15], and optical-force [16], have been used for their operation. Miniaturized actuators are also expected to produce a new type of haptic display for blind people and for internet shopping to transmit product information (for example, text and surface condition of a product).

Makishi, et al. developed a small-sized actuator based on a shape-memory alloy spring and produced a palm-top sized haptic display system for use of blind people [9]. The total size is 25 x 25 x 80 mm. The arrayed pins are individually driven up and down in a vertical direction. However, the system has disadvantages in that the size is still large and the structure is complicated. Gu, et al. proposed a braille display based on a piezoelectric type actuator [10]. This system can drive up its pins large power and large strokes. This method does not enable a reduction in the total size of the system because the micro actuator is enlarged to put out large power. Yoshikawa, et al. proposed a novel type of mm-sized haptic display [7]. They used micromachined beam structures and deposited a shape-memory alloy film on it to reduce the size of the display. The device can be used in tactile displays for internet shopping. The displacement and generative force produced are 30 μ m and 4.2 mN, respectively. The device has an advantage in that it can drastically reduce the volume of the system, however, the device's actuation method has to be improved to generate a larger force. MEMS technologies are now able to produce micro-sized actuators an arrayed manner for haptic displays. However difficulties will be experienced when trying to obtain relatively large generative forces required to operate haptic display applications if the



(b) Structure and operation principle of force transmission system for haptic displays
 Fig. 1 Schematic view and Principle of proposed arrayed vertical motion system.

size of the total system becomes smaller.

We previously proposed a novel type of arrayed vertical motion system to overcome this problem [17] (Fig.1). The system consists of an arrayed end-effector element, a clutch mechanism as the force and displacement transmitter, and a single mm-sized actuator as the large power and displacement generator, as shown in Fig. 1(b). The micro-machined clutch device selectively connects the power output from the mm-sized actuator to the arrayed end-effector element. The operation principle of the system is as follows: First, the clutch mechanism moves a block by using a tulip-shaped electrostatic actuator (Fig. 1(b-3)). Next, the mm-sized actuator lifts the power transmitter. When the block of the clutch mechanism meets the mesa structure of the arrayed end-effector element, the power and the displacement of the mm-sized actuator is transmitted to the end-effector element (Fig. 1(b-4)). Figure 2 shows the schematic view and the photograph of fabricated "Tulip-shaped electrostatic clutch device". We are confirming this device drives by 180V.

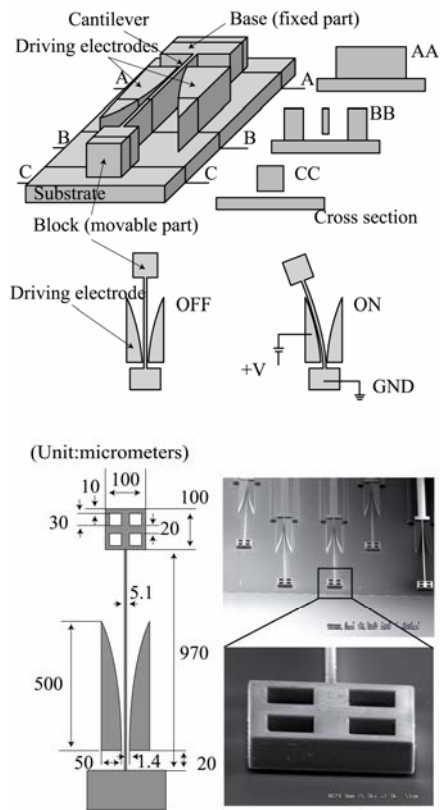


Fig. 2 Schematic view and fabricated “Tulip-shaped electrostatic actuator”.

The system is therefore able to obtain a large generative force because it uses a conventional mm-sized actuator and is able to drive the arrayed end-effector individually by using a selective connection on the electrostatic clutch device.

However, all the projection once move down (initial state) when the system drives different end effector element. The system has the drawback that it no able to move up the end effector element at different timing. The system has a drawback in that it cannot to move up the end-effector element at different timings. In this paper, we added a new electrostatic latch mechanism on the system so that the projection state could be controlled individually.

2. WORKING PRINCIPLE AND FABRICATION

The electrostatic latch mechanism to individually control the projection state during vertical motion is shown in Fig. 3. The mechanism was placed on the system and basically consists of an electrostatic latch plate and projection pins. The motion of the end-effector element is transmitted to a projection pin, and the pin is held on the latch plate by using electrostatic forces (Fig. 3(b)).

The electrical potential of the projection pins is zero because we applied +V and -V to each electrode respectively.

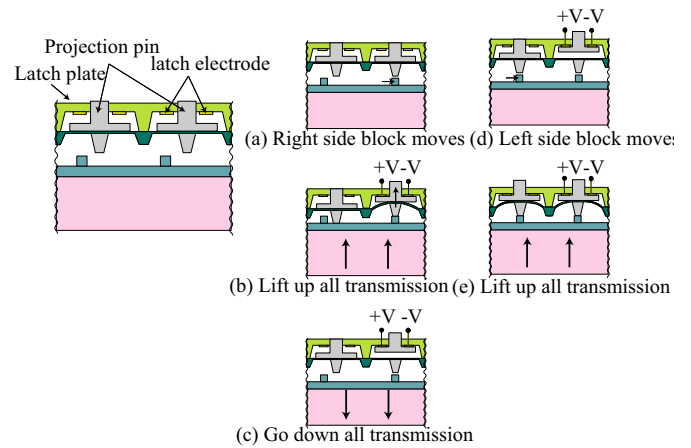


Fig. 3 Principle of arrayed vertical motion system with electrostatic latch system.

The system is, therefore, able to actuate different projection pins by keeping the previous state (Figs. 3(c), 3(d), and 3(e)).

We used MEMS technologies to fabricate the electrostatic latch mechanism. The process to fabricate the latch mechanism is shown in Fig. 4. We formed a recessed Si structure by applying KOH anisotropic wet etching (Figs. 4(a) and 4(b)). A SiO₂ layer was used as a masking material. An etched depth of 56 μm corresponded to the stroke of the projection pin. We used a glass plate as an insulator to form the electrode pattern for the latch. The holes were formed on a glass plate by using a mechanical drill, and the Cr/Au electrodes were patterned by using a lift-off process (Figs. 4(c) and 4(d)). Two substrates were bonded together by using a glass adhesive. We coated the bonded structure by using parylene film to form an insulation layer on the surface (Fig. 4(e)). The base of the projection pin was separated by mechanical dicing (Fig. 4(f)), and the cylinders were placed into the hole in the glass plate (Fig. 4(g)).

Figure 5 shows the dimensions and photographs of each part in the fabricated electrostatic latch mechanism. The diameter and length of the cylinder were 300 μm and 600 μm, respectively. We formed a 4x4 array electrostatic latch. The total size was 6.0 x 6.0 x 0.5 mm.

3. LATCH PERFORMANCE

We evaluated the relationship between the applied voltage and the electrostatic holding device (Fig. 6). The load was applied to one end of a beam, and the relationship was calculated from the deflection of the beam. The experimental results are shown in Fig. 7.

The force increased proportionally with the square of the applied voltage, and a holding force of a few mN was obtained for the spring device. We then theoretically calculated the relationship between applied voltage and the electrostatic force to compare with the experimentally

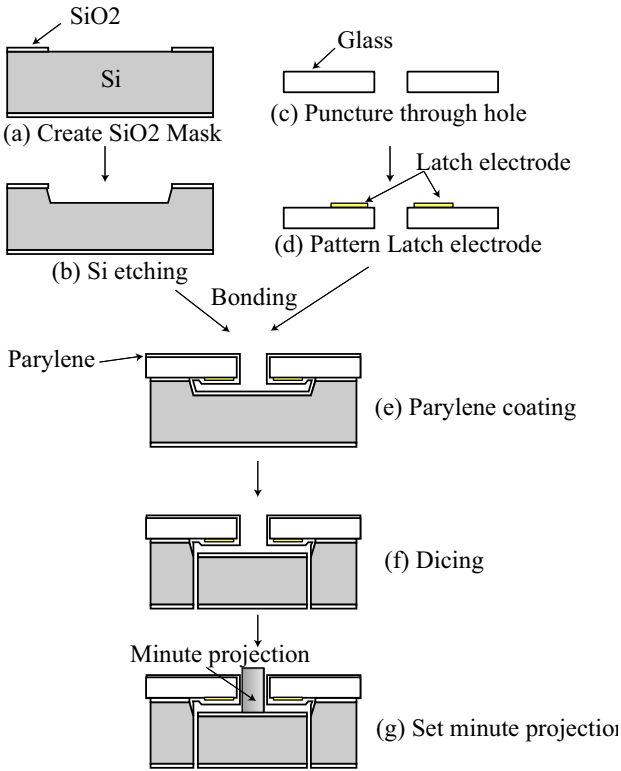


Fig. 4 Fabrication process of electrostatic latch system.

obtained force values.

The projection stand grips the latch plate by electrostatic force. When the latch electrode and the stand have stuck completely smoothly and ideally, the gripping power is shown by the next expression (1).

$$F = \frac{\epsilon_0 \epsilon_d S V^2}{2d^2} \quad (1)$$

When, gripping power F , electric constant ϵ_0 , area S , voltage V , relative permittivity ϵ_d , insulating layer thickness d .

However, a minute gap exists because the latch plate and the projection stage surface are rough. Therefore, the gripping power is shown by the next expression (2) when assuming that there is a constant gap between the latch electrode and the stand.

$$F = \frac{\epsilon_0 \epsilon_{air} S V^2}{2(d_g + \frac{d}{\epsilon_d})^2} \quad (2)$$

When, relative permittivity ϵ_{air} and air gap d_g .

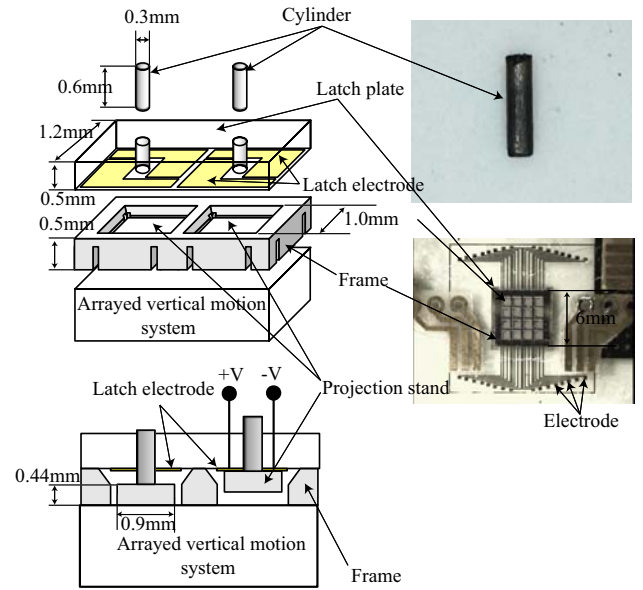


Fig. 5 Fabricated electrostatic latch system.

We then theoretically calculated the relationship between air-gap and the electrostatic force. The model used in the calculation and the obtained results are shown in Fig. 8.

The force obtained in the experiment was 2.48 mN when the applied voltage was 100 V. By using the obtained results and information from the graph, we assume that there is almost 3.43 μm gap between the latch that we can reduce the gap by improving the surface flatness of the latch plate to increase the electrostatic gripping force.

The developed electrostatic latch mechanism will be mounted on arrayed vertical motion systems, as shown in Fig. 9, in the future works.

4. CONCLUSION

We added a new electrostatic latch mechanism to the system to control the projection state individually. We used MEMS technologies to fabricate a 4x4 array electrostatic latch mechanism. The total size was 6.0 x 6.0 x 0.5 mm. We evaluated the relationship between the applied voltage and the electrostatic holding force by using a double cantilever spring device. The force proportionally increased proportionally with the square of the applied voltage, and a holding force of a few mN was obtained for the spring device.

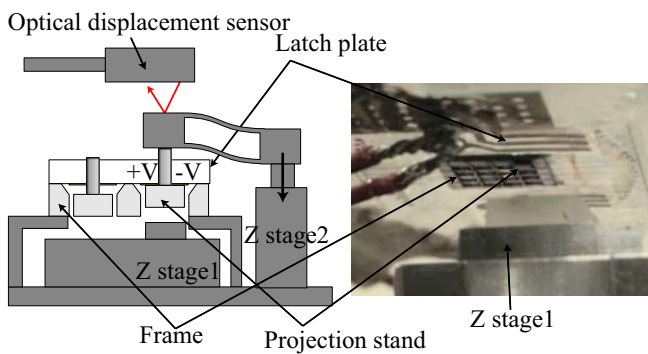


Fig. 6 Experimental set up

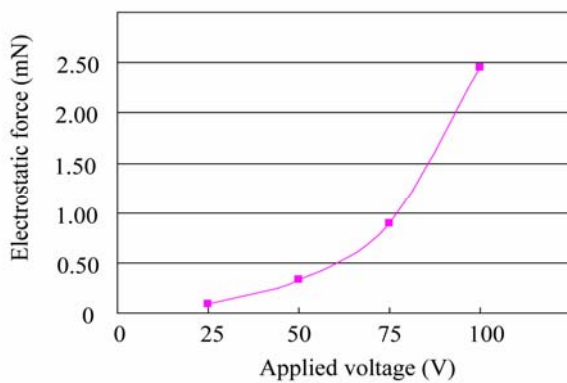


Fig. 7 Relationship between voltage and electrostatic force.

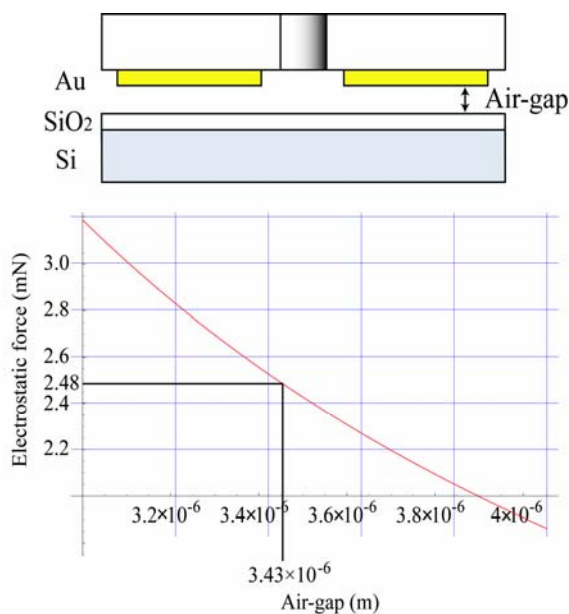


Fig. 8 Relationship between air-gap and electrostatic force.

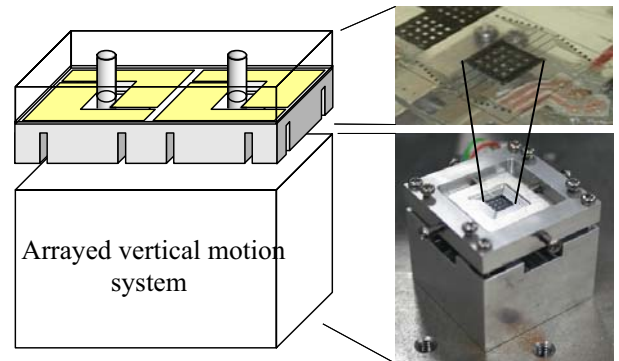


Fig. 9 Electrostatic latch mechanism mounted on arrayed vertical motion systems.

ACKNOWLEDGEMENTS

We would like to thank Dr. Nobuaki Kawahara, Mr. Yukihiro Takeuchi, and Mr. Junji Oohara, of DENSO Corp. for their useful suggestions and their help with our experiments. This work was supported by the 21st COE Program (Micro- and Nano-Mechatronics for Information-based Society)

REFERENCES

- [1] Bullen D and Liu C 2006 Electrostatically actuated dip pen nanolithography probe arrays *Sensors Actuators A* **125** 504–11
- [2] Suh J W, Glander S F, Darling R B, Stormont C W and Kovacs G T A 1997 Organic thermal and electrostatic ciliary microactuator array for object manipulation *Sensors Actuators A* **58** 51–60
- [3] Singh J, Gan T, Agarwal A, Mohanraj and Liw S 2005 3D free space thermally actuated micromirror device *Sensors Actuators A* **123–124** 468–75
- [4] Chen W-C, Chu C-C, Hsieh J and Fang W 2003 A reliable single-layer out-of-plane micromachined thermal actuator *Sensors Actuators A* **103** 48–58
- [5] Noworolski J M, Klaassen E H, Logan J R, Petersen K E and Maluf N I 1996 Process for in-plane and out-of-plane single-crystal-silicon thermal microactuators *Sensors Actuators A* **55** 65–6
- [6] Jain A, Qu H, Todd S and Xie H 2005 A thermal bimorph micromirror with large bi-directional and vertical actuation *Sensors Actuators A* **122** 9–15
- [7] Yoshikawa W, Sasabe A, Sugano K, Tsuchiya T, Tabata O and Ishida A 2006 Vertical drive micro actuator using SMA thin film for a smart button *MEMS2006 Technical Digest* pp 734–7
- [8] Feustel A, Krusemark O and Müller J 1998 Numerical simulation and optimization of planar electromagnetic actuators *Sensors Actuators A* **70** 276–82
- [9] Makishi W, Iwami K, Haga Y and Kawasaki M E 2001 Batch fabrication of SMA actuated pin display for blind aid *Technical Digest of the 18th Sensor Symposium* pp 137–42

- [10] Wei G, Zhu X, Futai N, Cho B S and Takayama S 2004 Computerized microfluidic cell culture using elastomeric channels and Braille displays *Proc. Natl Acad. Sci.* **101** 15861–6
- [11] Lam K H, Wang X X and Chan H L W 2006 Lead-free piezoceramic cymbal actuator *Sensors Actuators A* **125** 393–7
- [12] Zhang D-Y, Ono T and Esashi M 2005 Piezoactuator-integrated monolithic microstage with six degrees of freedom *Sensors Actuators A* **122** 301–6
- [13] Kim K Y, Park K H, Park H C, Goo N S and Yoon K J 2005 Performance evaluation of lightweight piezo-composite actuators *Sensors Actuators A* **120** 123–9
- [14] Kim Y-S, Nam H-J, Cho S-M, Hong J-W, Kim D-C and Bu J U 2003 PZT cantilever array integrated with piezoresistor sensor for high speed parallel operation of AFM *Sensors Actuators A* **103** 122–9
- [15] Juuti J, Lozinski A and Leppävuori S 2004 LTCC compatible PLZT thick-films for piezoelectric devices *Sensors Actuators A* **110** 361–4
- [16] Ha J-L, Kung Y-S, Hu S-C and Fung R-F 2006 Optimal design of a micro-positioning Scott–Russell mechanism by Taguchi method *Sensors Actuators A* **125** 565–72
- [17] H. Sasaki, M. Shikida, and K. Sato, “A force transmission system based on a tulip-shaped electrostatic clutch for haptic display devices”, *J. Micromech. Microeng.*, 16, pp. 2673-2683, 2006.